

EXPERIMENTAL STUDIES OF MICROARCS BETWEEN COPPER ELECTRODES IN AIR

J. K. C. BALLENTIN^{a,*}, M. BAEVA^b, D. UHRLANDT^{a,b}

^a *Institute for Electrical Engineering, University of Rostock, Rostock, Germany*

^b *Leibnitz Institute for Plasma Science and Technology, Greifswald, Germany*

* jonas.ballentin@uni-rostock.de

Abstract. Low direct current arcs generated between Cu electrodes in atmospheric pressure air are investigated in relation to low-voltage switching. Electrical and optical measurements and high-speed imaging give insight into the dynamics of the arc. Side-on spectroscopy with a grating spectrometer and suitable optical imaging delivers spatially resolved spectral emission coefficients of three emission lines of the Cu atom. The experimental findings are compared with results from modelling.

Keywords: Microarc, low-voltage circuit-breaker, copper electrodes, plasma spectroscopy.

1. Introduction

The increasing use of direct current (DC) applications in the low-voltage (LV) regime, which is up to 1500V, is caused by the growing demand on the renewable energy supply infrastructure with solar cells, fuel cells, and batteries. Contrary to alternating current (AC), DC has no natural zero-crossing, which makes the switching and breaking of currents more complicated. The fast extinction of microarcs remains a crucial part of the switching process and is therefore essential for the development of safer, smaller, cheaper and environmentally friendlier switching devices. Due to insufficient galvanic disconnection and conduction with comparable high resistances in semi-conducting switching devices, the utilization of mechanical contact separation is hardly avoidable.

Stand-alone electrical measurements give already insights into the microarcs, however, the derived black-box models are not generalisable since the model parameters are strongly dependent on the breaker construction itself [1, 2]. Therefore, sophisticated plasma models complemented with electric circuit and the electrode models (including heat transfer, release of metal atoms and electron emission mechanisms) are currently under development [1, 3]. It is expected that such models are capable of predicting plasma parameters like the electric potential, temperatures and number densities of heavy particles and electrons.

We investigate microarcs in the low current regime (1–10 A), where a key characteristic is their deviation from local thermodynamic equilibrium (LTE), making them more difficult to describe than arcs at higher currents and larger electrode gaps, which tend to exhibit equilibrium properties. With that, this work contributes to the general understanding of non-equilibrium plasmas.

Since the plasma composition strongly influences the electrical conductivity, it plays an important role in the characterization of the microarcs under considera-

tion. A crucial aspect here is the presence of metal atoms released from the electrodes, because their ionization potential (e.g. 7.7 eV for Cu) is well below that of typical filling gas components such as N₂ and O₂. With spatially and temporally resolved measurements of the plasma radiation, this work aims to provide data supporting the development of the unified non-equilibrium plasma model.

2. Experimental Setup

To reproduce the physical conditions of a typical LV DC current breaker, the microarc is generated between two separating Cu electrodes in atmospheric pressure air. A signal generator with an amplifier in the current mode produces pulses of constant current at 2–5 A. A step motor is used to set one electrode in a reproducible motion, while the position of the second electrode is fixed. During the opening process, the microarc voltage is measured using a digital oscilloscope (Yokogawa DLM2054), while a high-speed camera (Photron Fast-Cam NOVA R3) captures the emitted light in the visible range with a frame rate of 1000 s⁻¹ and a minimal exposure is 2 μs.

Side-on optical emission spectroscopy (OES) is performed in order to get insight into the arc radiation. For this purpose, the arc is imaged onto a grating spectrometer with an entrance slit of 20 μm width. This ensures that the emission from a 'slice' of the arc is analysed. The side-on spectrum is captured with a 10³ × 10³ CCD of a PI-Max4:1024i with exposure time of around 0.1 ms. The axial position of observation is adjusted using a linear translation stage, on which the electrode setup with the motor is mounted (figure 1). In order to ensure that the arc has a certain length at the moment of capturing the spectrum, the triggering is synchronized with the motor operation.

The high-speed camera is equipped with an in-house built dual imaging system (DIS) that enables the simultaneous capturing of two synchronized videos

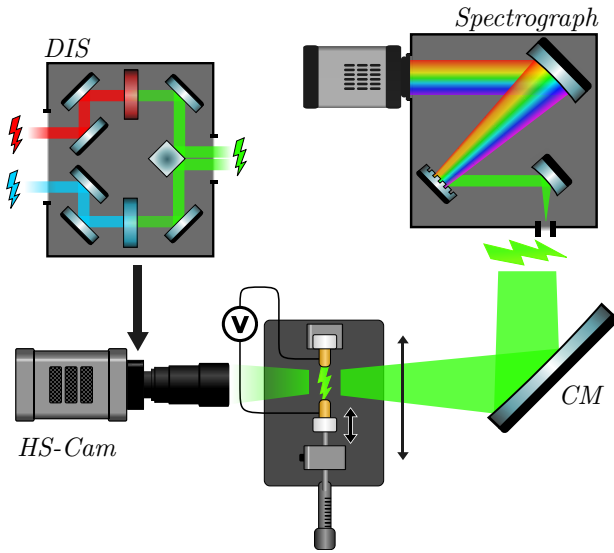


Figure 1. Scheme of the experimental setup with the high-speed camera (HS-Cam), the concave mirror (CM) for imaging, the spectrograph, and the dual imaging system (DIS) containing spectral filters.

from the same perspective and the observation of the spectral dynamics. It comprises eight planar mirroring surfaces for image doubling (see figure 1) and is placed between the CMOS image sensor and the lens of the camera. Two narrow band metal interference filters are inserted into the module so that records of two emission lines from the arc are made. The filter transmittances are chosen to be centred at the Cu I emission line at 515 nm (filter band width of 1 nm) and the O I triplet at 777 nm (2 nm filter band width), respectively.

3. Collisional-radiative model

A previously developed unified non-equilibrium model [3] is used to obtain the plasma parameters in air-Cu mixture in comparison with experimental findings [4]. This is a one-dimensional (1D) fluid model, which includes the ground state atoms and singly charged ions of Cu are considered along with the 11-species reaction scheme for air. The model solves the equations for conservation of species, energy of electrons and heavy particles (atoms, molecules, ions), the Poisson equations for the electric potential, the heat transfer in the electrodes for a current level controlled by an external circuit. The contribution of the excited Cu-states to the ionization is taken into account applying the modified diffusion approximation. In this work, we extend the basic model to a collisional-radiative model in order to obtain the population of the excited states. Species equations are solved for levels and groups of levels with plasma parameters known from the basic model. These levels/groups with the corresponding energies and statistical weights are as follows: $4s^2\ ^2D_{5/2}$ (1.39 eV, 6), $4s^2\ ^2D_{3/2}$ (1.64 eV, 4), $4^2P_{1/2}$ (3.79 eV, 2), $4^2P_{3/2}$ (3.82 eV, 4), Cu($4^1P^0, 4^1D^0, 4^1F^0$) (5.20 eV, 60), $5^2S_{1/2}$ (5.35 eV, 2), Cu($5^2P_{1/2}, 5^2P_{3/2}$, and $4^2D_{3/2}$,

$4^2D_{5/2}$) (6.17 eV, 16). Processes of electron impact excitation, ionization, and spontaneous emission are considered with cross-section data and transition probabilities from [5, 6].

4. Results and discussion

4.1. Emission coefficients

The side-on spectroscopy returns the spectral radiance for all side-on positions y during a fixed time of contact separation for a fixed axial position z . Three emission lines of Cu I (wavelengths of 510.6 nm, 515.3 nm, and 521.8 nm) were investigated. For the spectral analysis, the two dimensional raw data containing a spectral and radial component is subdivided into radial units, in which the spectra are evaluated individually, i.e., each emission line is fitted with a Voigt-profile that yields the integrated over the wavelength intensity I . The obtained intensity at each side-on unit are further fitted to an intensity profile $I(y)$. A Gaussian function with an offset has proven to be the most suitable fit for the radial profile. The result for an arc with a length of 3 mm at a DC current of 2 A is shown in figure 2a for the axial position of 300 μ m from the anode. Assuming that the plasma is cylindrically symmetric and optically thin (no self-absorption) - both assumptions are reasonable under the real arc conditions - the radial profile of the emission coefficient $\varepsilon(r)$ can be numerically reconstructed applying Abel inversion of $I(y)$ (see figure 2b). Since the investigated transitions originate from different energy levels, an estimate of the excitation temperature $T_{\text{ex}} = 4500\text{--}6000$ K and the number density of Cu atoms of $n_{\text{Cu}} = 10^{21}\text{--}10^{22}$ m $^{-3}$ are obtained employing the Boltzmann plot approach. T_{ex} should represent the electron temperature provided the excitation occurs in collisions with electrons. Note that both appear to increase in the near electrode regions (not shown here). However, because of the deviation from LTE, further analysis in detail that would require equilibrium conditions is not pursued.

For the sake of comparison with the 1D collisional-radiative model, an average emission coefficient is evaluated by dividing the radial mean intensity with the arc radius. The spectral emission coefficient is related to the number density of the upper level n_k as

$$\varepsilon_\lambda = \frac{hc}{4\pi\lambda_{ki}} A_{ki} n_k, \quad (1)$$

where A_{ki} and λ_{ki} are respectively the transition probability and the wavelength of the transition $k \rightarrow i$. The calculated mean densities are compared with those from the model in figure 3 for different axial positions in the arc. The experimental data indicate a decrease of the number densities in the middle of the arc by about an order of magnitude, while the decrease in the simulation results is stronger pronounced. Note that the discharge radius in the model is considered to increase with the gap length and adjusted to match the measured voltage. Furthermore, the evaluated

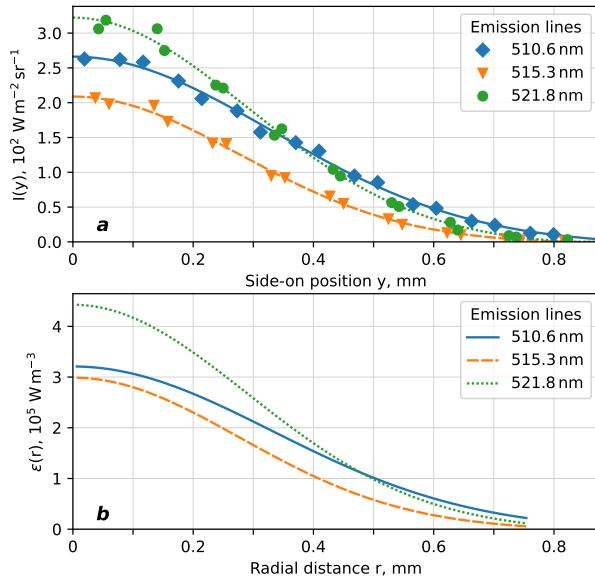


Figure 2. The intensities $I(y)$ measured at a distance of $300\mu\text{m}$ from the anode and the reconstructed emission coefficients $\varepsilon(r)$ of the arc for a gap distance of 3mm and DC current of 2A .

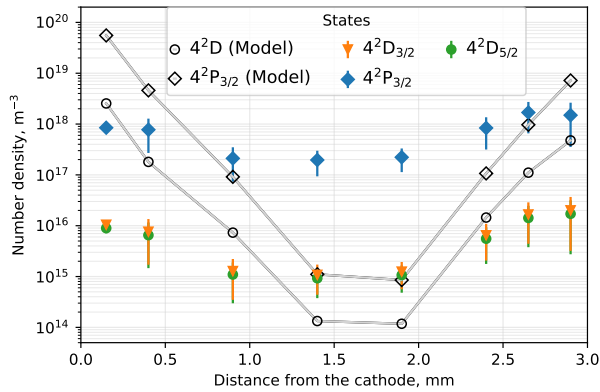


Figure 3. Radially averaged number density of excited levels from experiment and modelling.

emission coefficients vary by an order of magnitude from one measurement to the next, regardless if the measurement is done near an electrode or in the centre of the discharge gap. This indicates a highly dynamic nature of the arc plasma, which is discussed in the following.

4.2. Arc dynamics

To capture the arc dynamics, measurements of the arcs voltage have been synchronized with the high-speed DIS. Figure 4 shows the images of the Cu I (515 nm) and O I (777 nm) emission of the arc recorded at two instants (33 ms and 34 ms), for which the gap length is approximately 1.5mm . The images show that the arc emission is stronger near the electrodes (the anode on the left and the cathode on the right hand side). The O I emission is brightest at the cathode, while the Cu I emission can be on the anode side as well. The

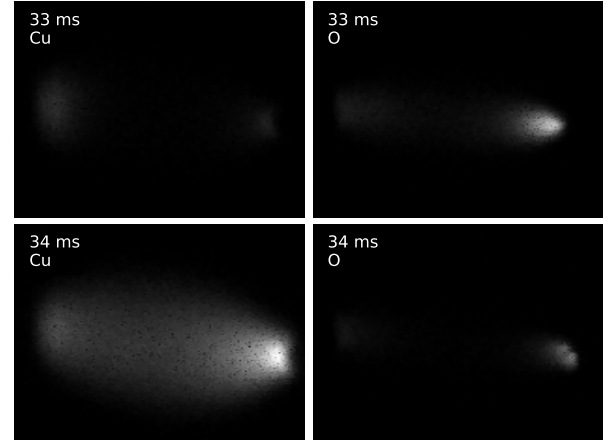


Figure 4. Dual imaging with spectral filters for Cu I and O I emission lines at two instants. The cathode is on the right hand side. The images measure $1.40 \times 1.55\text{mm}$, the acquisition time is 1ms .

observations show that the anode spot is mostly quite static, while the cathode spot changes its location very frequently. Multiple cathode spots can appear simultaneously in experiments with exposure times of less than $100\mu\text{s}$ (see the image with O I at the instant of 34 ms).

The emission from the whole arc in the corresponding spectral ranges is considered during the opening process for the sake of a more detailed investigation of the arc dynamics. All pixel values of a given frame are summed up to an intensity value for a given instant. The dynamics of the arc emission as synchronized with the arc voltage is shown in figure 5. At the beginning, the voltage immediately jumps to about 15V that can be associated with the sheath voltage. The further increase of the arc voltage during the opening is due to the voltage drop in the plasma bulk. The Cu I emission exhibits the above mentioned dynamic fluctuations of up to one order of magnitude. An inverse relationship between the Cu I and O I emission is observed. While the Cu I emission increases, the O I emission reduces. At the same time, the arc voltage slightly decreases. These effects can be seen in figure 5 quiet well at the instants of about 34 ms and 57 ms.

This behaviour can be interpreted as follows. When Cu metal vapour is released from the electrodes into the plasma, the number densities of Cu^+ ions and electrons increase due to low ionization potential of Cu. The latter is roughly about the half that of the air components. The higher number density of charge carriers in the discharge enlarges the arc conductivity so that the voltage is reduced. Simultaneously, less electron energy is available for exciting O atoms, as the Cu radiation facilitates energy transport out of the plasma.

4.3. Contact opening in the model

The contact separation is implemented in the non-equilibrium model [4] employing a deforming mesh

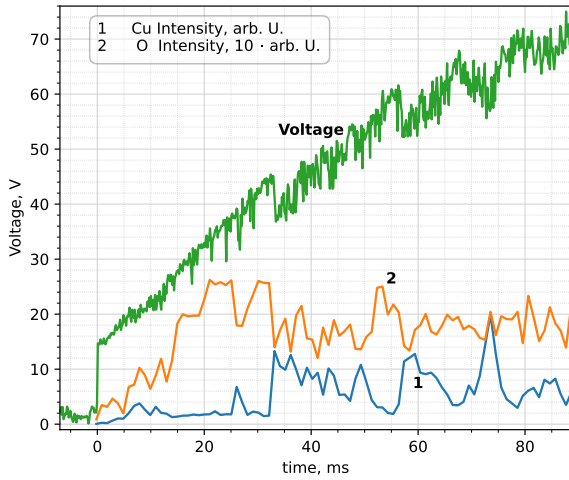


Figure 5. Voltage and whole arcs intensity of a Cu I and O I line during the contact opening. The contact separation starts at $t=0$.

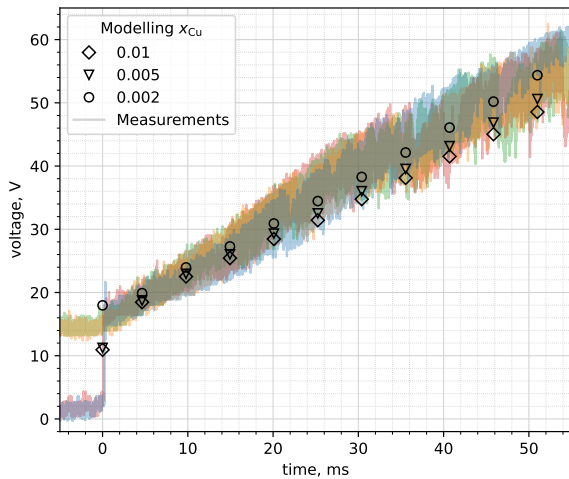


Figure 6. Arc voltage during the contact opening for various Cu mole fractions x_{Cu} in the air-Cu mixture. The contact separation starts at $t=0$.

of the plasma region. Parametric studies have been performed, in which the discharge radius, the field enhancement factor in the evaluation of the therm-field electron emission from the Cu cathode, and the mole fraction of Cu in the air-Cu mixture were varied. The results for a field enhancement factor of 140 Cu mole fractions x_{Cu} of 0.01, 0.005, 0.002 are shown in figure 6 along with some experimental results. The microarc is initially burning in a gap of 30 μm for 11 ms. The further increase of the gap length up to 3 mm starts at $t=0$ and takes 51 ms. Note that the model predicts the previously discussed observation, i.e., a significant increase in the Cu mole fraction (factor of five) is accompanied by a decrease of the arc voltage by more than ten percent.

5. Conclusions

Microarcs generated between separating Cu electrodes in atmospheric pressure air have been studied at low

DC currents by means of optical emission spectroscopy, high-speed imaging with narrow spectral filters, and electrical measurements.

Side-on emission spectra for an arc gap length of 3 mm arcs have been recorded. The radial distribution of the emission intensity of the Cu I lines at 510.6 nm, 515.3 nm, and 521.8 nm has been obtained for various axial positions. Assuming that the plasma is cylindrically symmetric and optically thin, the corresponding emission coefficients and the number density of the upper levels have been obtained.

The results from the high-speed imaging of the arc demonstrate the dynamic behaviour of the arc. They further reveal a correlation between a rise of the Cu I emission intensity (515.3 nm) and a decrease of the O I emission intensity (777 nm) and the arc voltage.

First results from a 1D unified non-equilibrium and a collisional-radiative models are compared with the experimental findings. The computed arc voltage during the contact opening and parametric studies with various mole fraction of Cu in the air-Cu mixture match well the experimental results.

Acknowledgements

The work is funded by the German Research Foundation (DFG) Project number 524731006.

Data availability statement The data that support the findings of this study are openly available at the following URL/DOI: <https://doi.org/10.34711/INPTDAT.972>.

References

- [1] D. Uhrlandt, A. Najam, G. Gött, et al. Electrical models of arcs in different applications. *Plasma Phys. Technol.*, 11(1):28–35, 2024. [doi:10.14311/ppt.2024.1.28](https://doi.org/10.14311/ppt.2024.1.28).
- [2] A. Najam, P. Pieterse, and D. Uhrlandt. Electrical modelling of switching arcs in a low voltage relay at low currents. *Energies*, 13(23), 2020. [doi:10.3390/en13236377](https://doi.org/10.3390/en13236377).
- [3] M. Baeva and D. Uhrlandt. Modelling of microarcs in copper metal vapour dominated air. *J. Phys. D: Appl. Phys.*, 58(9):095204, 2024. [doi:10.1088/1361-6463/ad9f79](https://doi.org/10.1088/1361-6463/ad9f79).
- [4] M. Baeva, J. K. C. Ballentin, and D. Uhrlandt. Modelling studies of arcs of short length between copper electrodes (submitted). *Plasma Phys. Technol.*, 12(1):40, 2025. [doi:10.14311/ppt.2025.1.40](https://doi.org/10.14311/ppt.2025.1.40).
- [5] A. Bogaerts, R. Gijbels, and R. J. Carman. Collisional-radiative model for the sputtered copper atoms and ions in a direct current argon glow discharge. *Spec. Acta Part B: At. Spec.*, 53(12):1679–1703, 1998. [doi:10.1016/S0584-8547\(98\)00201-8](https://doi.org/10.1016/S0584-8547(98)00201-8).
- [6] I. Babich, V. Boretskij, A. Veklich, and R. Semenyshyn. Spectroscopic data and stark broadening of Cu I and Ag I spectral lines: Selection and analysis. *Adv. Space Res.*, 54(7):1254–1263, 2014. [doi:10.1016/j.asr.2013.10.034](https://doi.org/10.1016/j.asr.2013.10.034).